Synergies between QCD global analysis and LQCD JAM examples

Nobuo Sato

Parton Distributions and Lattice Calculations (PDFLattice 2024)
Jefferson Lab, Nov 18, 2024

Jefferson Lab

Outline

1. Gluon helicity PDF
2. Nucleon transversity/tensorcharge
3. Pion PDF

Outline

1. **Gluon helicity PDF**
2. Nucleon transversity/tensorcharge
3. Pion PDF

Zhou, NS, Melnitchouk ‘22
Karpie, Whitehill, Melnitchouk, Monahan, Orginos, Qiu, Richards, NS, Zafeiropoulos ‘23
Hunt-Smith, Cocuzza, Melnitchouk, NS, Thomas, White ‘24

Zhou, Melnitchouk, NS '21

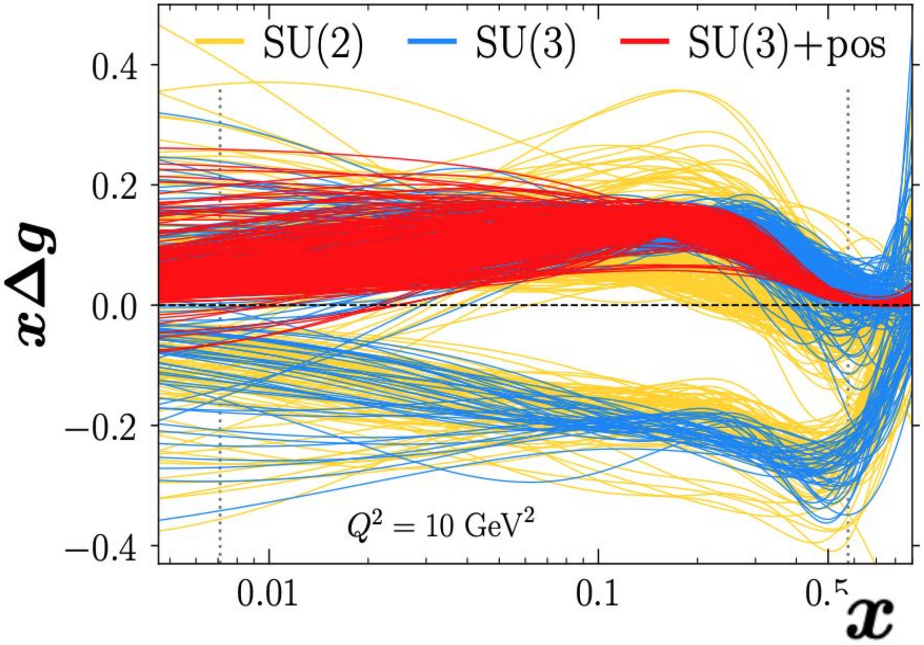

$$|\Delta g| < g$$

PDF positivity constraint

- Sign of gluon-hpdf is not uniquely determined by existing experimental data (DIS W^2 > 10 GeV^2)
- PDF positivity constraints + data strongly disfavors negative g-hpdf
- Negative g-hpdf violates significantly pdf positivity constraint
- PDF positivity is not a strict requirement in QCD

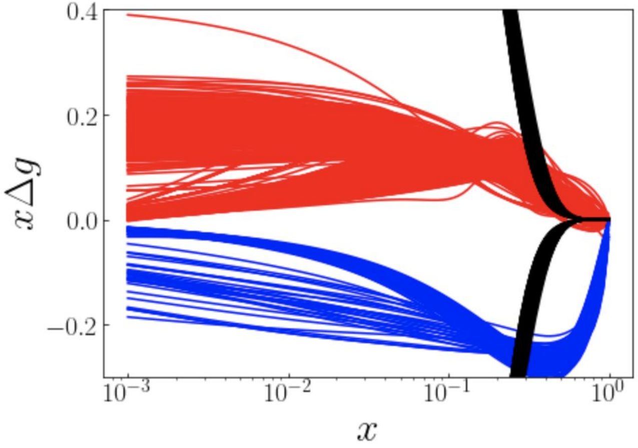

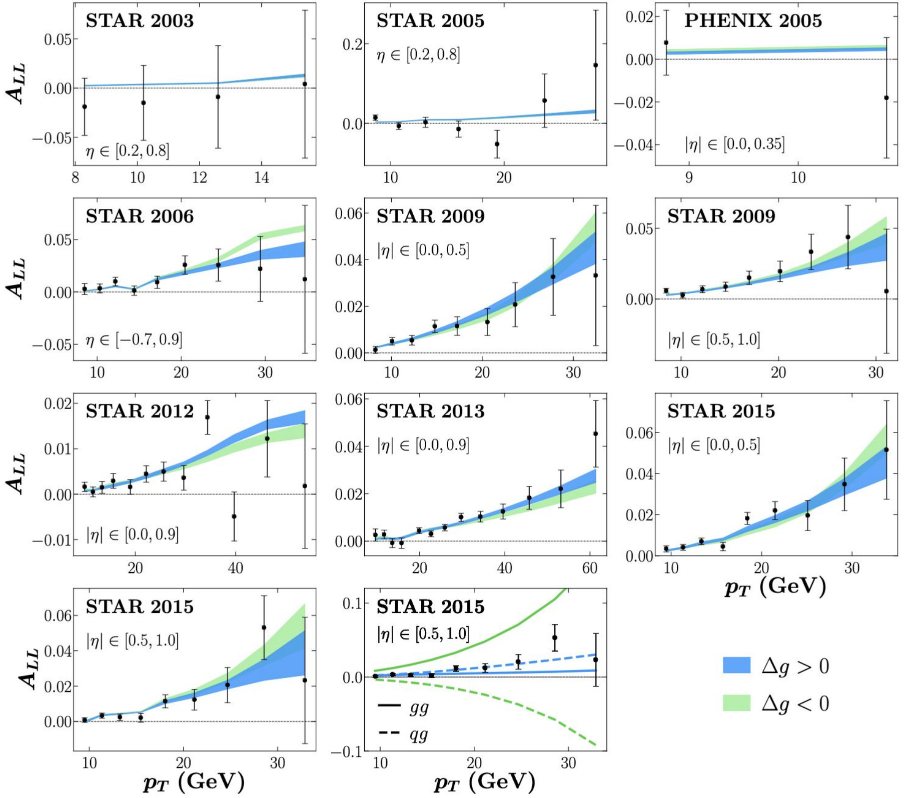

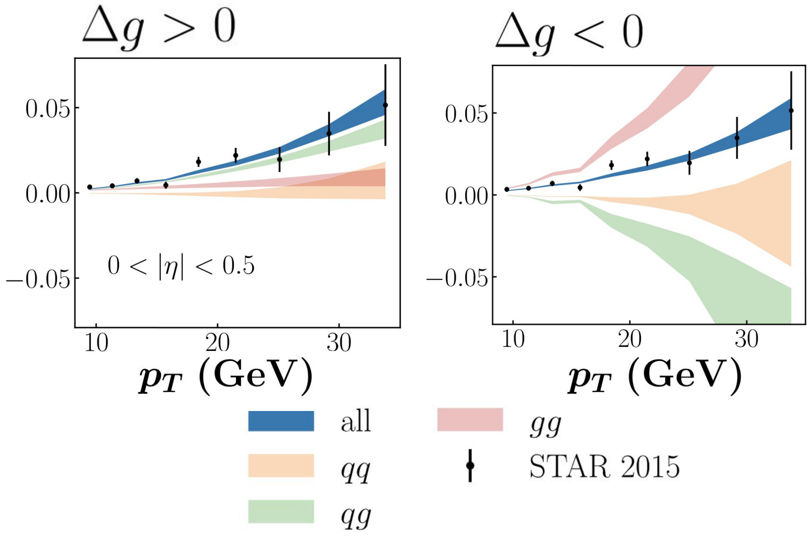

$$A_{LL}^{\text{jet}}(p_T, y) \;\propto\; a_{gg}[\Delta g \otimes \Delta g] + \sum_q a_{qg}[\Delta q \otimes \Delta g] + \sum_{q,q'} a_{qq'}[\Delta q \otimes \Delta q'] \;+\; \mathcal{O}(\alpha_s),$$

$$|A_{LL}| < 1$$ ✓

g-hpdf enters quadratically, and different subchannels contribute with different signs and strengths

Measurement of charged pion double spin asymmetries at midrapidity in longitudinally polarized $p + p$ collisions at $\sqrt{s}$ = 510 GeV

PHENIX Collaboration • U.A. Acharya (Georgia State U.) et al. (Apr 6, 2020)

Published in: *Phys.Rev.D* 102 (2020) 3, 032001 • e-Print: 2004.02681 [hep-ex]

Charged-pion cross sections and double-helicity asymmetries in polarized p+p collisions at $\sqrt{s}$=200 GeV

PHENIX Collaboration • A. Adare (Colorado U.) et al. (Sep 5, 2014)

Published in: *Phys.Rev.D* 91 (2015) 3, 032001 • e-Print: 1409.1907 [hep-ex]

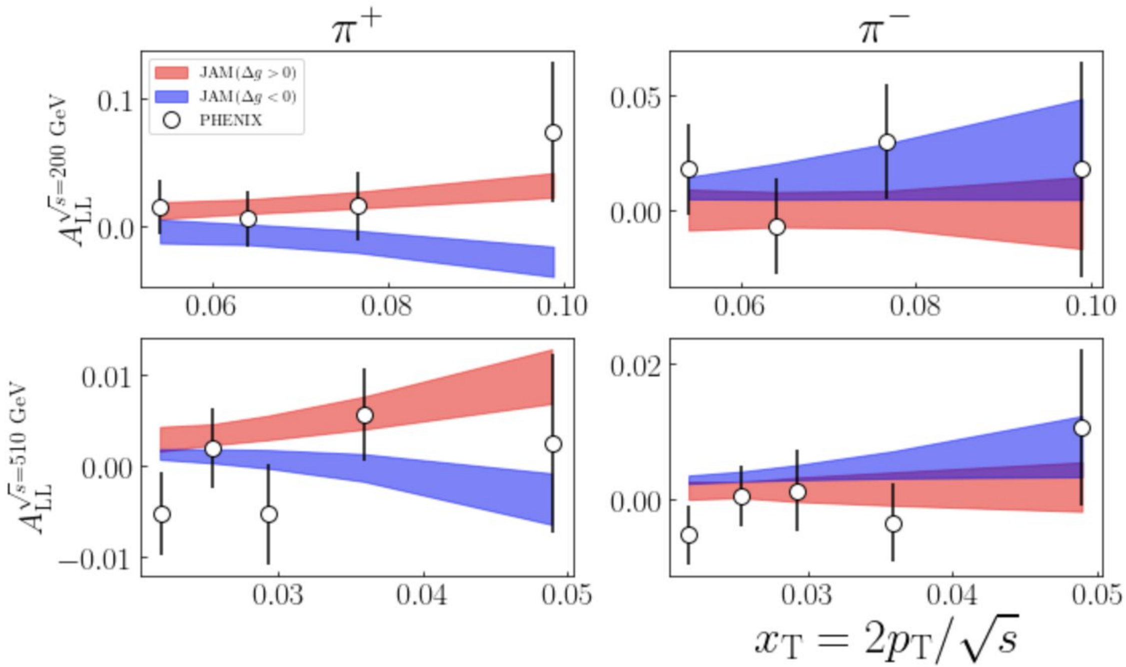

- PHENIX collaboration stated that the gluon spin contribution is positive
- The two solutions for g-hpdf found by JAM describe the data equally well

Measurement of Direct-Photon Cross Section and Double-Helicity Asymmetry at $\sqrt{s} = 510$ GeV in $\vec{p} + \vec{p}$ Collisions

PHENIX Collaboration • U. Acharya (Georgia State U., Atlanta) et al. (Feb 16, 2022)

e-Print: 2202.08158 [hep-ex]

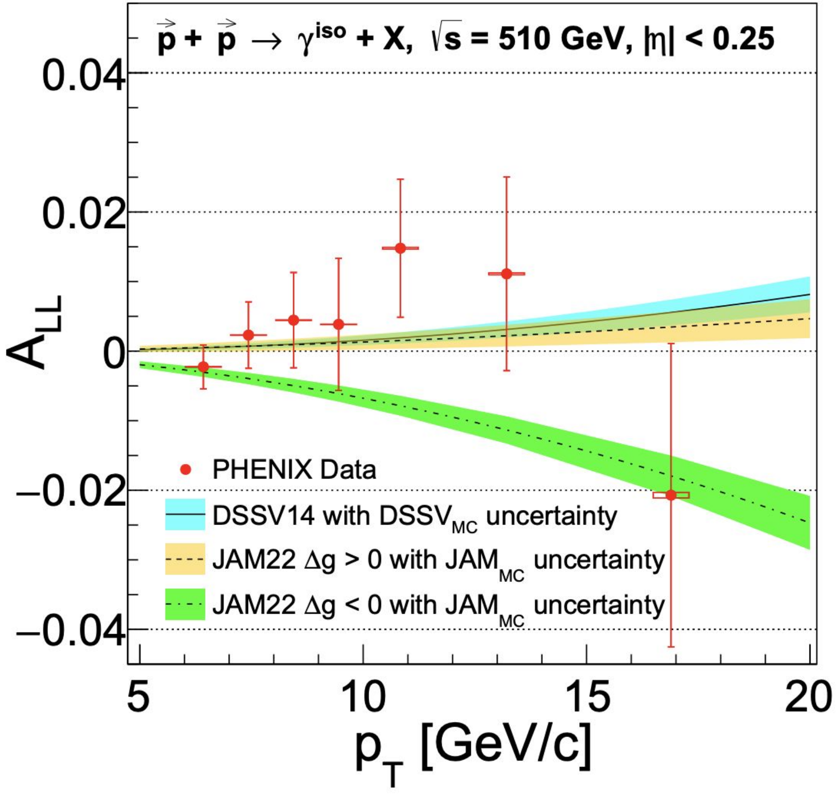

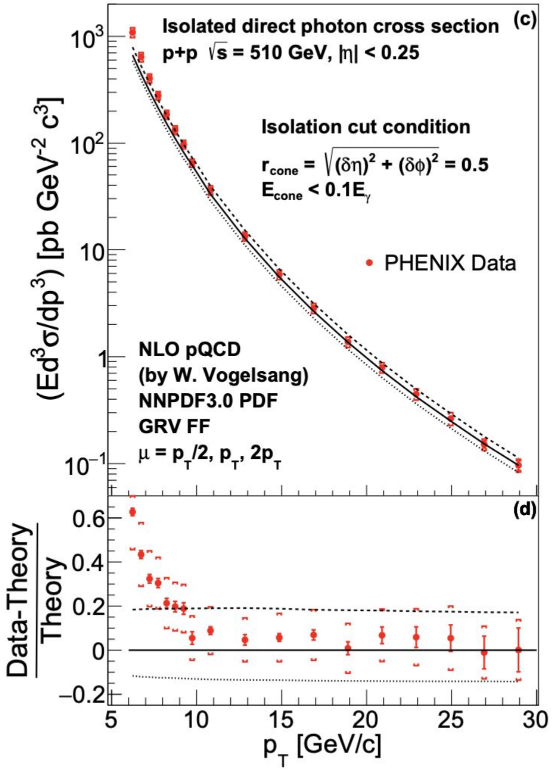

- PHENIX collaboration stated that negative g-hpdf is disfavored by more than 2.8 σ
- However, only last 3 high-pT A_LL points are well described in pQCD (see denominator of A_LL)

Toward the determination of the gluon helicity distribution in the nucleon from lattice quantum chromodynamics

HadStruc Collaboration • Colin Egerer (Jefferson Lab) et al. (Jul 18, 2022)

Published in: *Phys.Rev.D* 106 (2022) 9, 094511 • e-Print: 2207.08733 [hep-lat]

$$\widetilde{M}^{\mu\nu;\alpha\beta}(p,z) = \langle p|F^{\mu\nu}(0)W(0;z)\widetilde{F}^{\alpha\beta}(z)|p\rangle$$

$$\widetilde{\mathfrak{M}}(\nu,z^2) = \frac{\widetilde{M}_{00}(p,z)/p_0p_3Z_L(z_3/a)}{M_{00}(p=0,z)/m^2}$$

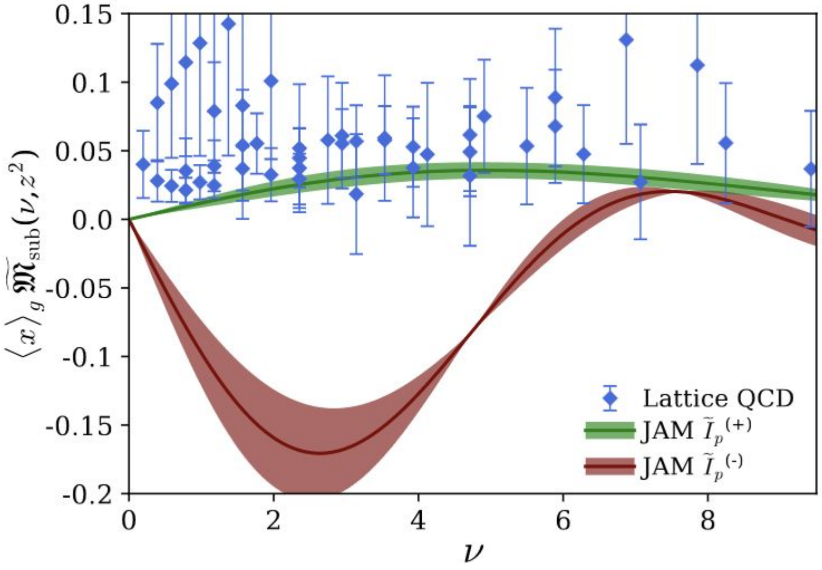

$$\begin{aligned}\widetilde{\mathfrak{M}}(\nu,z^2)\langle x_g\rangle_{\mu^2} =\ & \widetilde{\mathcal{I}}_p(\nu,\mu^2) - \frac{\alpha_s N_c}{2\pi}\int_0^1 \mathrm{d}u\,\widetilde{\mathcal{I}}_p(u\nu,\mu^2)\Bigg\{\ln\left(z^2\mu^2\frac{e^{2\gamma_E}}{4}\right)\\ & \left(\left[\frac{2u^2}{\bar{u}}+4u\bar{u}\right]_+ - \left(\frac{1}{2}+\frac{4}{3}\frac{\langle x_S\rangle_{\mu^2}}{\langle x_g\rangle_{\mu^2}}\right)\delta(\bar{u})\right)\\ & + 4\left[\frac{u+\ln(1-u)}{\bar{u}}\right]_+ - \left(\frac{1}{\bar{u}}-\bar{u}\right)_+ - \frac{1}{2}\delta(\bar{u}) + 2\bar{u}u\Bigg\}\\ & - \frac{\alpha_s C_F}{2\pi}\int_0^1 \mathrm{d}u\,\widetilde{\mathcal{I}}_S(u\nu,\mu^2)\left\{\ln\left(z^2\mu^2\frac{e^{2\gamma_E}}{4}\right)\widetilde{\mathcal{B}}_{gq}(u) + 2\bar{u}u\right\} + \mathcal{O}(\Lambda^2_{\rm QCD}z^2)\,,\end{aligned}$$

$$\widetilde{\mathcal{I}}_p(\nu) = \frac{i}{2}\int_{-1}^{1}\mathrm{d}x\, e^{-ix\nu}\, x\,\Delta g(x)\,.$$

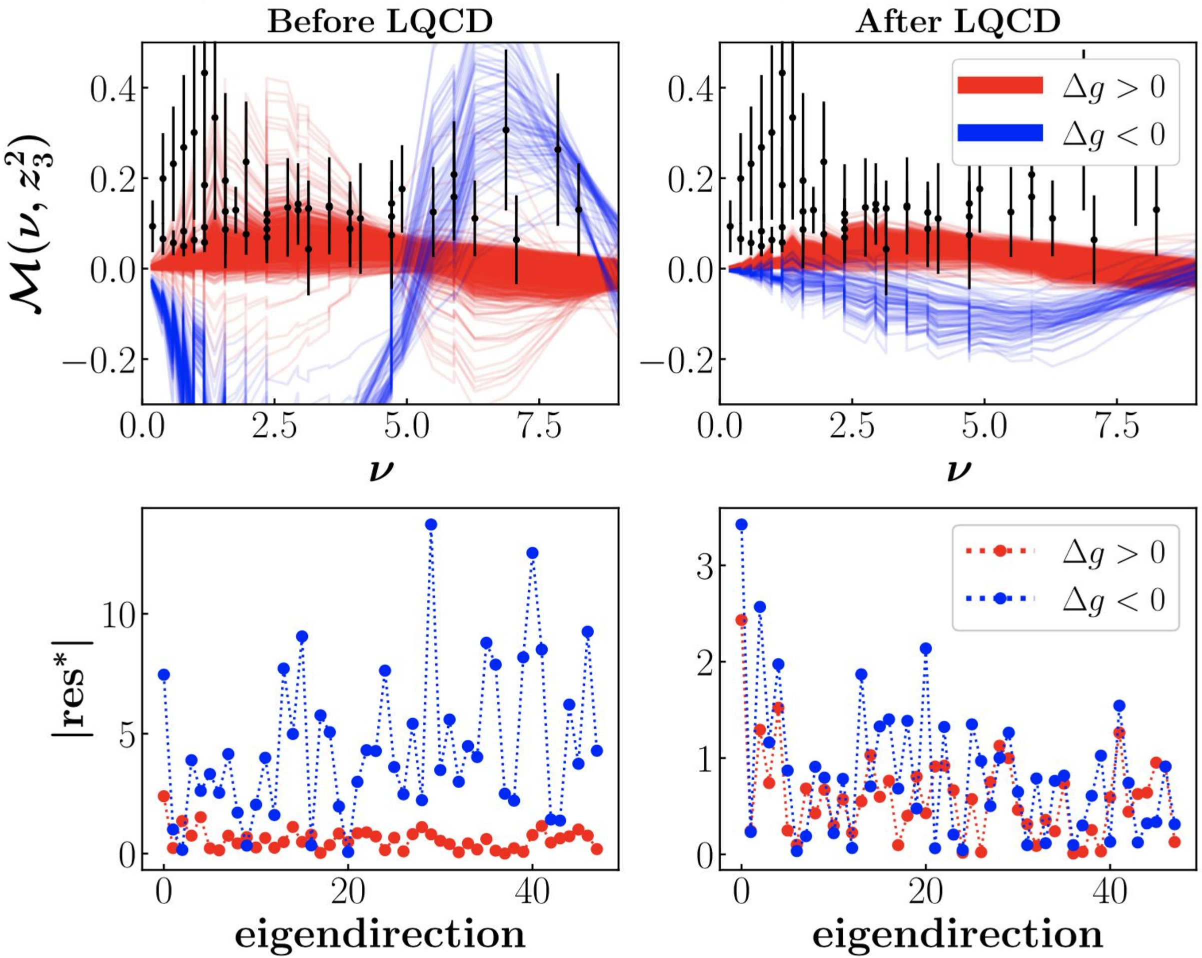

$$
\begin{aligned}
\chi^2 &= (\boldsymbol{d} - \boldsymbol{t})^T \boldsymbol{\Sigma}^{-1} (\boldsymbol{d} - \boldsymbol{t}) \\
&= (\boldsymbol{d} - \boldsymbol{t})^T \boldsymbol{U} \boldsymbol{D}^{-1} \boldsymbol{U}^T (\boldsymbol{d} - \boldsymbol{t}) \\
&= \sum_i \mathrm{res}_i^{*2}.
\end{aligned}
$$

- PCA projections of residuals reveal strong correlations between LQCD data points
- The correlations prevent determination of g-hpdf sign

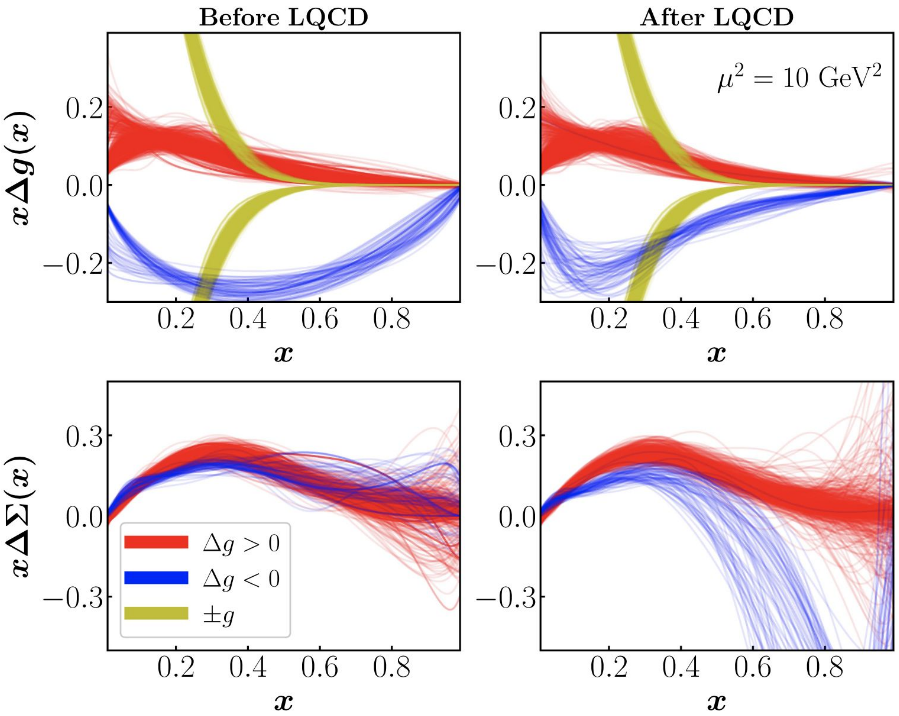

- LQCD distorts significantly the negative g-hpdf at higher x > 0.3
- Note that both solutions violate pdf positivity bounds for x > 0.3
- Before inclusion of LQCD data, singlet-hpdf were stable for both solutions
- Inclusion of LQCD data forces the quark singlet-hpdf to become negative at x > 0.4 for the negative g-hpdf

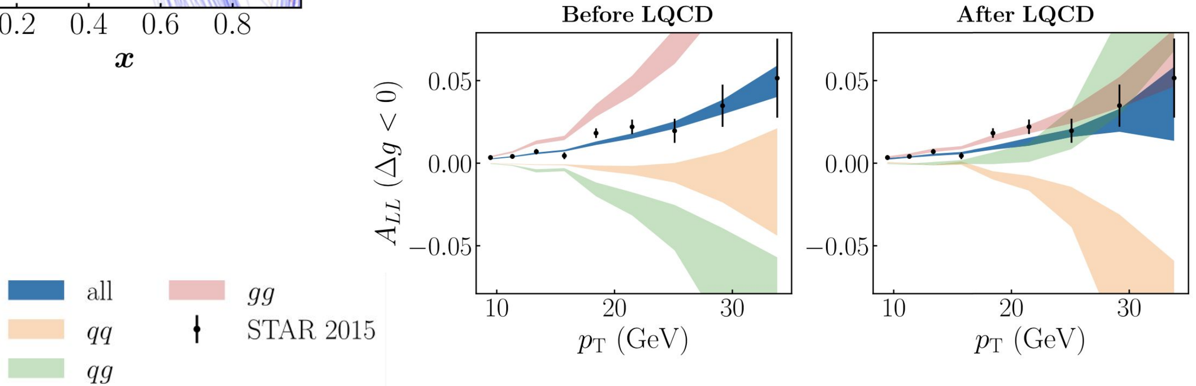

Higgs production at RHIC and the positivity of the gluon helicity distribution

Daniel de Florian[a], Stefano Forte[b], Werner Vogelsang[c]

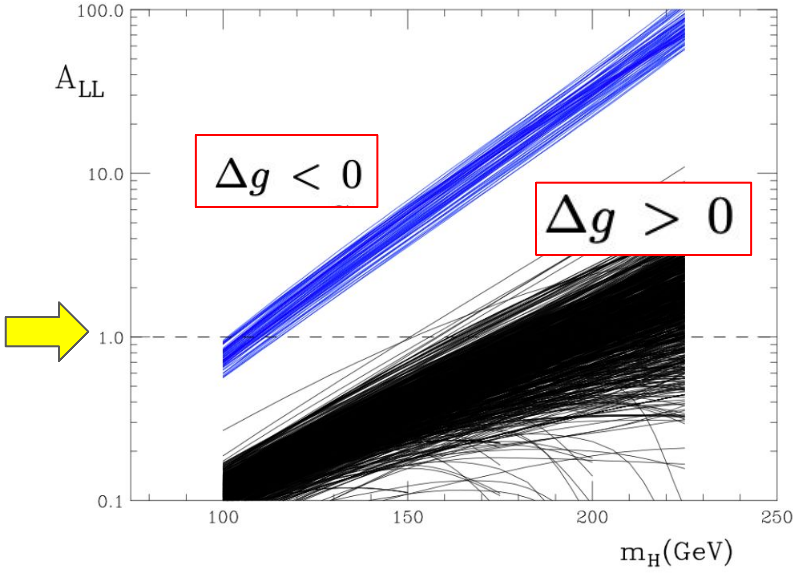

- Higgs A_LL is directly sensitive to g-hpdf squared at LO
- Calculations of A_LL(H) with negative g-hpdf can lead to unphysical results

$$A^{\rm H}_{LL}(\tau) = \frac{[\Delta g \otimes \Delta g]}{[g \otimes g]} + \mathcal{O}(\alpha_s),$$

Can Higgs A_LL fully discriminate negative g-hpdf?

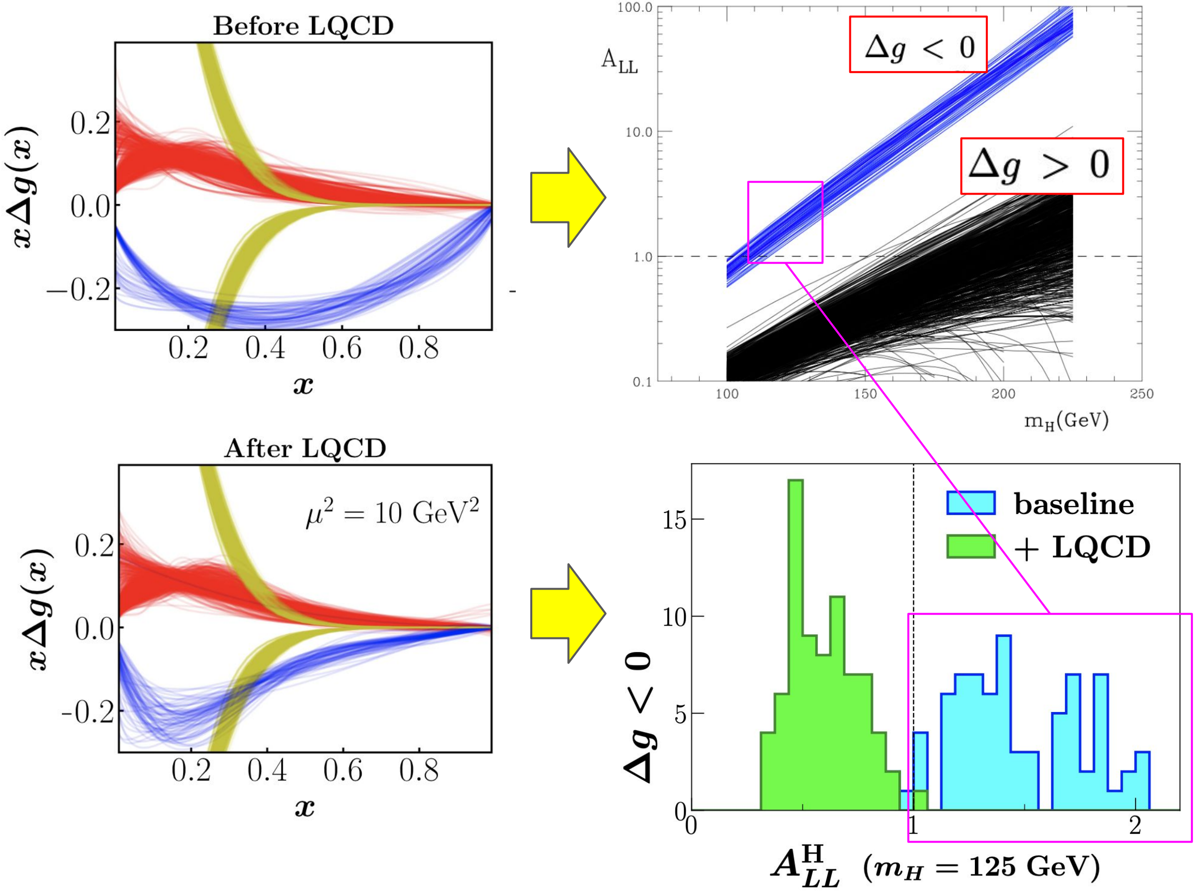

Negative g-hpdf with LQCD constraints still admits a physical Higgs A_LL

Physical Review Letters

Highlights Recent Accepted Collections Authors Referees Press About Editorial T

OPEN ACCESS | GO MOBILE » | ACCESS BY SURA JEFFERSON LABORATORY

New Data-Driven Constraints on the Sign of Gluon Polarization in the Proton

N. T. Hunt-Smith[1], C. Cocuzza[2], W. Melnitchouk[3], N. Sato[3], A. W. Thomas[1], and M. J. White[1] (JAM Collaboration-Spin PDF Analysis Group)

Show more

1370 additional data points for pol DIS (+ high-x DIS)

	$\chi^2_{\rm red}(\Delta g > 0)$			$\chi^2_{\rm red}(\Delta g < 0)$			N
Reaction	baseline	+ LQCD	+ high-x DIS	baseline	+ LQCD	+ high-x DIS	
Polarized							
Inclusive DIS	0.95	0.96	1.21	0.98	1.12	1.25	1735*
SIDIS	0.85	0.84	1.08	0.84	0.96	1.11	231
Inclusive jets	0.84	0.89	0.90	0.88	1.10	1.44	83
Inclusive $W^{\pm}/Z$	0.60	0.60	0.99	0.83	0.84	1.32	18
Total	**0.89**	**0.90**	**1.18**	**0.92**	**1.06**	**1.24**	**2067**
Unpolarized							
Inclusive DIS	1.17	1.17	1.17	1.18	1.18	1.19	3908
SIDIS	0.99	0.99	1.04	0.99	0.99	1.02	1490
Inclusive jets	1.28	1.28	1.30	1.29	1.29	1.30	198
Drell-Yan	1.21	1.21	1.21	1.24	1.24	1.24	205
Inclusive $W^{\pm}/Z$	1.01	1.01	1.01	1.03	1.03	1.04	153
Total	**1.14**	**1.14**	**1.14**	**1.15**	**1.15**	**1.15**	**5954**
SIA	0.86	0.86	0.89	0.90	0.90	0.92	564
LQCD	—	0.57	0.58	—	1.18	3.92	48
Total	**1.08**	**1.10**	**1.13**	**1.10**	**1.12**	**1.17**	**8633**

Takeaways

- For the first time, we were able to discriminate the sign of g-hpdf using data-driven approach
- Constraints from LQCD along with DSAs from jets and DIS at large-x were crucial to achieve the resolution of g-hpdf sign
- Inclusion of LQCD is becoming increasingly important in global analysis
- Experimental constraints at large x on gluon - hpdf are still scarce, and more data needed to reach precision similar to unpolarized gluon density (EIC - small x, JLab12/22 - high x)

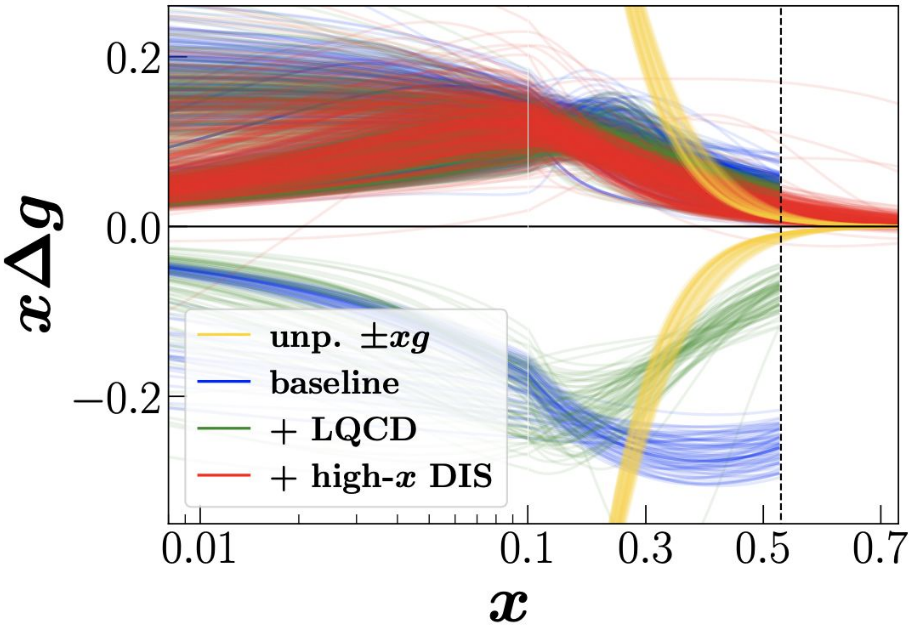

Outline

1. Gluon helicity PDF
2. **Nucleon transversity/tensorcharge**
3. Pion PDF

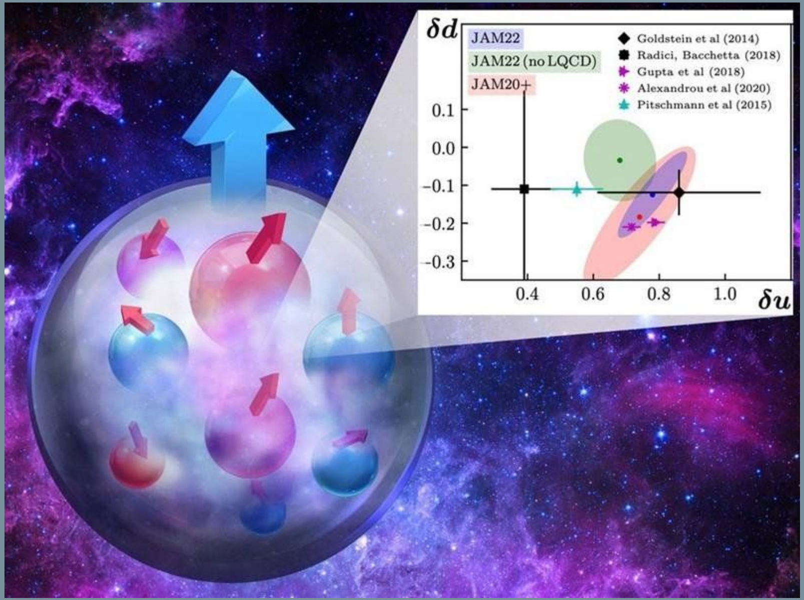

Pitonyak, Cocuzza, Metz, Prokudin, NS, `24 (PRL)
Cocuzza, Metz, Pitonyak, Prokudin, NS, Seidl `24 (PRL)
Cocuzza, Metz, Pitonyak, Prokudin, NS, Seidl `24 (PRD)

Gamberg, Malda, Miller, Pitonyak, Prokudin, NS, `22

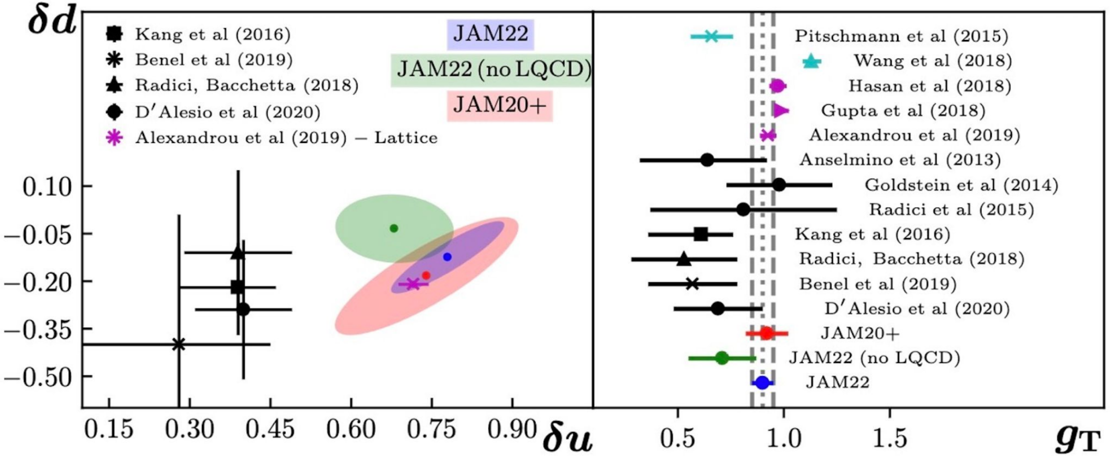

- TMD+CT3 pheno in tension with other analyzes (delta u)
- Radici, Bacchetta, and Benel, Courtoy, Ferro-Hernandez used collinear di-hadron observables to extract tensor charges
- New fresh look at collinear di-hadron pheno

Observable	Reactions	Non-Perturbative Function(s)	χ^2/npts	Exp. Refs.
$A_{UT}^{\sin(\phi_h-\phi_S)}$	$e+(p,d)^\uparrow \to e+(\pi^+,\pi^-,\pi^0)+X$	$f_{1T}^\perp(x,\vec{k}_T^2)$	$182.9/166=1.10$	[22, 24, 27]
$A_{UT}^{\sin(\phi_h+\phi_S)}$	$e+(p,d)^\uparrow \to e+(\pi^+,\pi^-,\pi^0)+X$	$h_1(x,\vec{k}_T^2), H_1^\perp(z,z^2\vec{p}_T^2)$	$181.0/166=1.09$	[22, 24, 27]
$^*A_{UT}^{\sin\phi_S}$	$e+p^\uparrow \to e+(\pi^+,\pi^-,\pi^0)+X$	$h_1(x), \tilde{H}(z)$	$18.6/36=0.52$	[22, 24, 27]
$A_{UC/UL}$	$e^+ + e^- \to \pi^+\pi^-(UC,UL)+X$	$H_1^\perp(z,z^2\vec{p}_T^2)$	$154.9/176=0.88$	[29–32]
$A_{T,\mu^+\mu^-}^{\sin\phi_S}$	$\pi^- + p^\uparrow \to \mu^+\mu^- + X$	$f_{1T}^\perp(x,\vec{k}_T^2)$	$6.92/12=0.58$	[34]
$A_N^{W/Z}$	$p^\uparrow + p \to (W^+,W^-,Z)+X$	$f_{1T}^\perp(x,\vec{k}_T^2)$	$30.8/17=1.81$	[35]
A_N^π	$p^\uparrow + p \to (\pi^+,\pi^-,\pi^0)+X$	$h_1(x), F_{FT}(x,x)=\frac{1}{\pi}f_{1T}^{\perp(1)}(x), H_1^{\perp(1)}(z), \tilde{H}(z)$	$70.4/60=1.17$	[7, 9, 10, 13]
Lattice g_T	——	$h_1(x)$	$1.82/1=1.82$	[89]

Collaboration	References	Observable	Process	Nonperturbative function(s)
Belle	[64]	$d\sigma/dz\, dM_h$	$e^+e^- \to (\pi^+\pi^-)X$	D_1
Belle	[112]	$A^{e^+e^-}$	$e^+e^- \to (\pi^+\pi^-)(\pi^+\pi^-)X$	$D_1, H_1^{\sphericalangle}$
HERMES	[118]	A_{UT}^{SIDIS}	$ep^\uparrow \to e'(\pi^+\pi^-)X$	$D_1, H_1^{\sphericalangle}, h_1$
COMPASS	[117]	A_{UT}^{SIDIS}	$\mu\{p, D\}^\uparrow \to \mu'(\pi^+\pi^-)X$	$D_1, H_1^{\sphericalangle}, h_1$
STAR	[97,121]	A_{UT}^{pp}	$p^\uparrow p \to (\pi^+\pi^-)X$	$D_1, H_1^{\sphericalangle}, h_1$
ETMC	[77]	$\delta u,\ \delta d$	LQCD	h_1
PNDME	[71]	$\delta u,\ \delta d$	LQCD	h_1

$$\frac{d\sigma}{dz\, dM_h} = \frac{4\pi N_c \alpha_{\text{em}}^2}{3s} \sum_q \bar{e}_q^2 D_1^q(z, M_h),$$

$$A^{e^+e^-}(z, M_h, \bar{z}, \bar{M}_h) = \frac{\sin^2\theta \sum_q e_q^2 H_1^{\sphericalangle,q}(z, M_h) H_1^{\sphericalangle,\bar{q}}(\bar{z}, \bar{M}_h)}{(1+\cos^2\theta)\sum_q e_q^2 D_1^q(z, M_h) D_1^{\bar{q}}(\bar{z}, \bar{M}_h)}$$

$$A_{UT}^{\text{SIDIS}} = c(y) \frac{\sum_q e_q^2 h_1^q(x) H_1^{\sphericalangle,q}(z, M_h)}{\sum_q e_q^2 f_1^q(x) D_1^q(z, M_h)}$$

$$A_{UT}^{pp} = \frac{2P_{hT} \sum_i \sum_{a,b,c,d} \int_{x_a^{\min}}^1 dx_a \int_{x_b^{\min}}^1 \frac{dx_b}{z} h_1^a(x_a) f_1^b(x_b) \frac{d\Delta\hat{\sigma}_{a^\uparrow b \to c^\uparrow d}}{d\hat{t}} H_1^{\sphericalangle,c}(z, M_h)}{2P_{hT} \sum_i \sum_{a,b,c,d} \int_{x_a^{\min}}^1 dx_a \int_{x_b^{\min}}^1 \frac{dx_b}{z} f_1^a(x_a) f_1^b(x_b) \frac{d\hat{\sigma}_{ab \to cd}}{d\hat{t}} D_1^c(z, M_h)}$$

→ $h_1(x; \mu^2)$ Transversity (TPDF)

$H_1^{\sphericalangle}(z, M_h; \mu^2)$ Interference FF (IFF)

$D_1(z, M_h; \mu^2)$ Dihadron FF (DiFFs)

Experiment	Binning	N_{dat}	χ^2_{red} JAMDiFF (w/ LQCD)	(no LQCD)	(SIDIS only)
Belle (cross section) [64]	z, M_h	1094	1.01	1.01	1.01
Belle (Artru-Collins) [112]	z, M_h	55	1.27	1.24	1.28
	$M_h, \overline{M}_h$	64	0.60	0.60	0.60
	$z, \bar{z}$	64	0.42	0.42	0.41
HERMES [118]	x_{bj}	4	1.77	1.70	1.67
	M_h	4	0.41	0.42	0.47
	z	4	1.20	1.17	1.13
COMPASS (p) [117]	x_{bj}	9	1.98	0.65	0.59
	M_h	10	0.92	0.94	0.93
	z	7	0.77	0.60	0.63
COMPASS (D) [117]	x_{bj}	9	1.37	1.42	1.22
	M_h	10	0.45	0.37	0.38
	z	7	0.50	0.46	0.46
STAR [121]	$M_h, \eta < 0$	5	2.57	2.56	
$\sqrt{s} = 200$ GeV	$M_h, \eta > 0$	5	1.34	1.55	
$R < 0.3$	$P_{hT}, \eta < 0$	5	0.98	1.00	
	$P_{hT}, \eta > 0$	5	1.73	1.74	
	η	4	0.52	1.46	
STAR [97]	$M_h, \eta < 0$	32	1.30	1.10	
$\sqrt{s} = 500$ GeV	$M_h, \eta > 0$	32	0.81	0.78	
$R < 0.7$	$P_{hT}, \eta > 0$	35	1.09	1.07	
	η	7	2.97	1.83	
ETMC δu [77]		1	0.71		
ETMC δd [77]		1	1.02		
PNDME δu [71]		1	8.68		
PNDME δd [71]		1	0.04		
Total χ^2_{red} (N_{dat})			**1.01** (1475)	**0.98** (1471)	0.96 (1341)

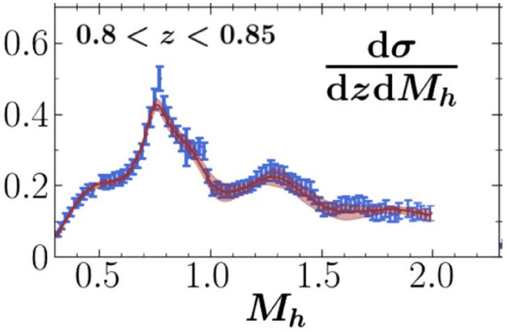

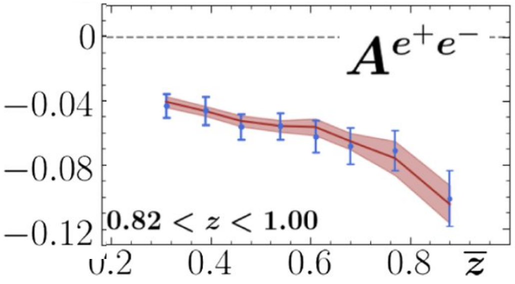

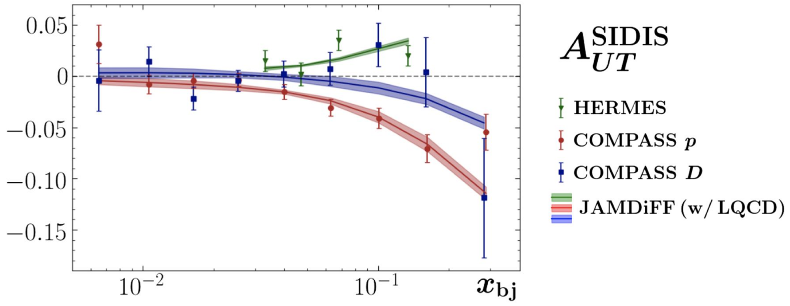

Reconstructed TPDF

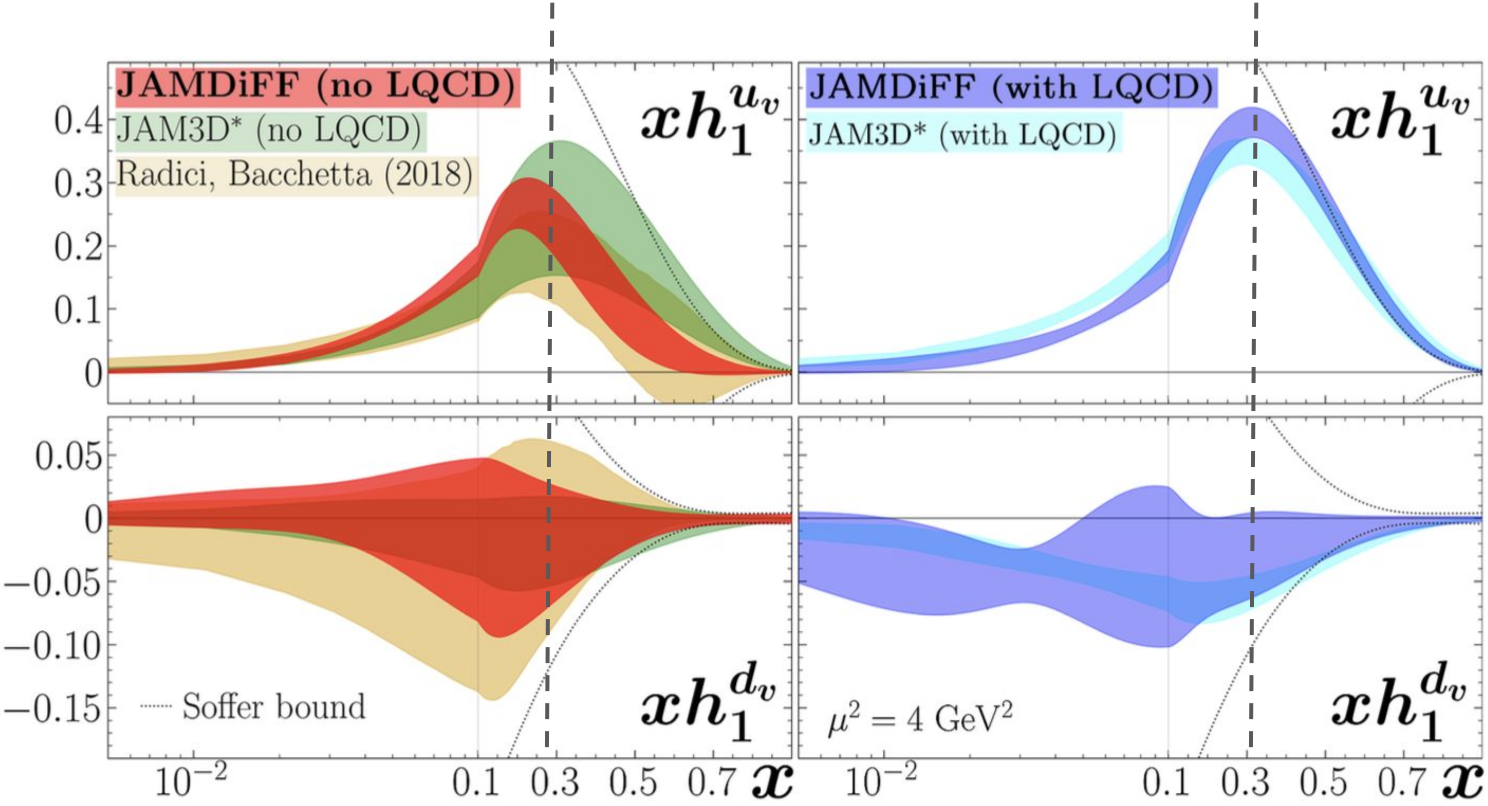

Reconstructed TPDF

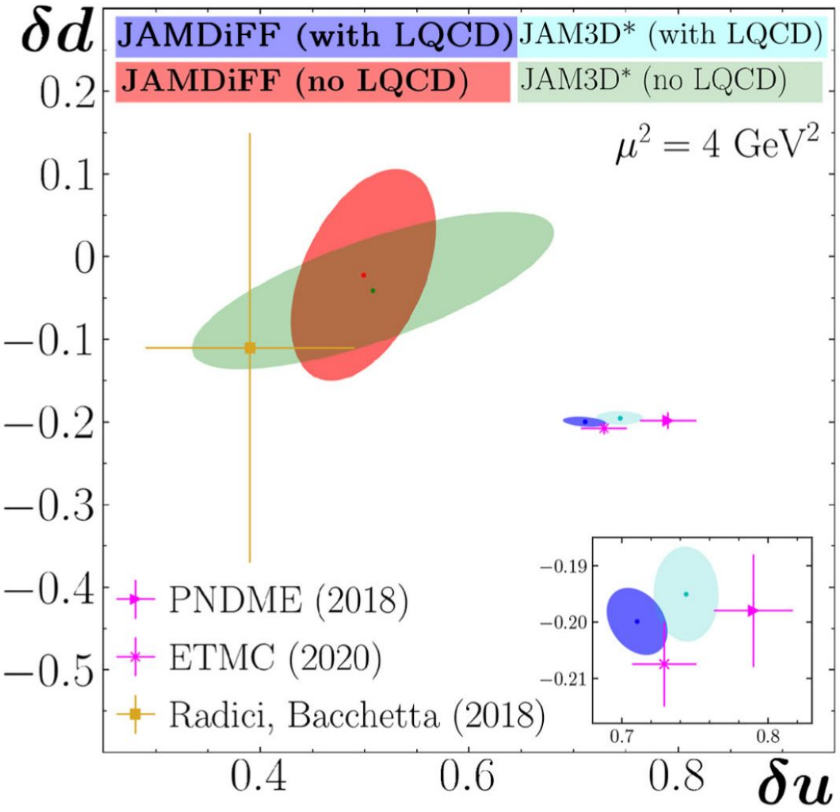

	χ^2_{red}	
	JAMDiFF	
Experiment	**(w/ LQCD)**	**(no LQCD)**
Belle (cross section) [64]	1.01	1.01
	1.27	1.24
Belle (Artru-Collins) [112]	0.60	0.60
	0.42	0.42
	1.77	1.70
HERMES [118]	0.41	0.42
	1.20	1.17
	1.98	0.65
COMPASS (p) [117]	0.92	0.94
	0.77	0.60
	1.37	1.42
COMPASS (D) [117]	0.45	0.37
	0.50	0.46
	2.57	2.56
STAR [121]	1.34	1.55
$\sqrt{s} = 200$ GeV	0.98	1.00
$R < 0.3$	1.73	1.74
	0.52	1.46
	1.30	1.10
STAR [97]	0.81	0.78
$\sqrt{s} = 500$ GeV	1.09	1.07
$R < 0.7$	2.97	1.83
ETMC δu [77]	0.71	
ETMC δd [77]	1.02	
PNDME δu [71]	8.68	
PNDME δd [71]	0.04	
Total χ^2_{red} (N_{dat})	**1.01** (1475)	**0.98** (1471)

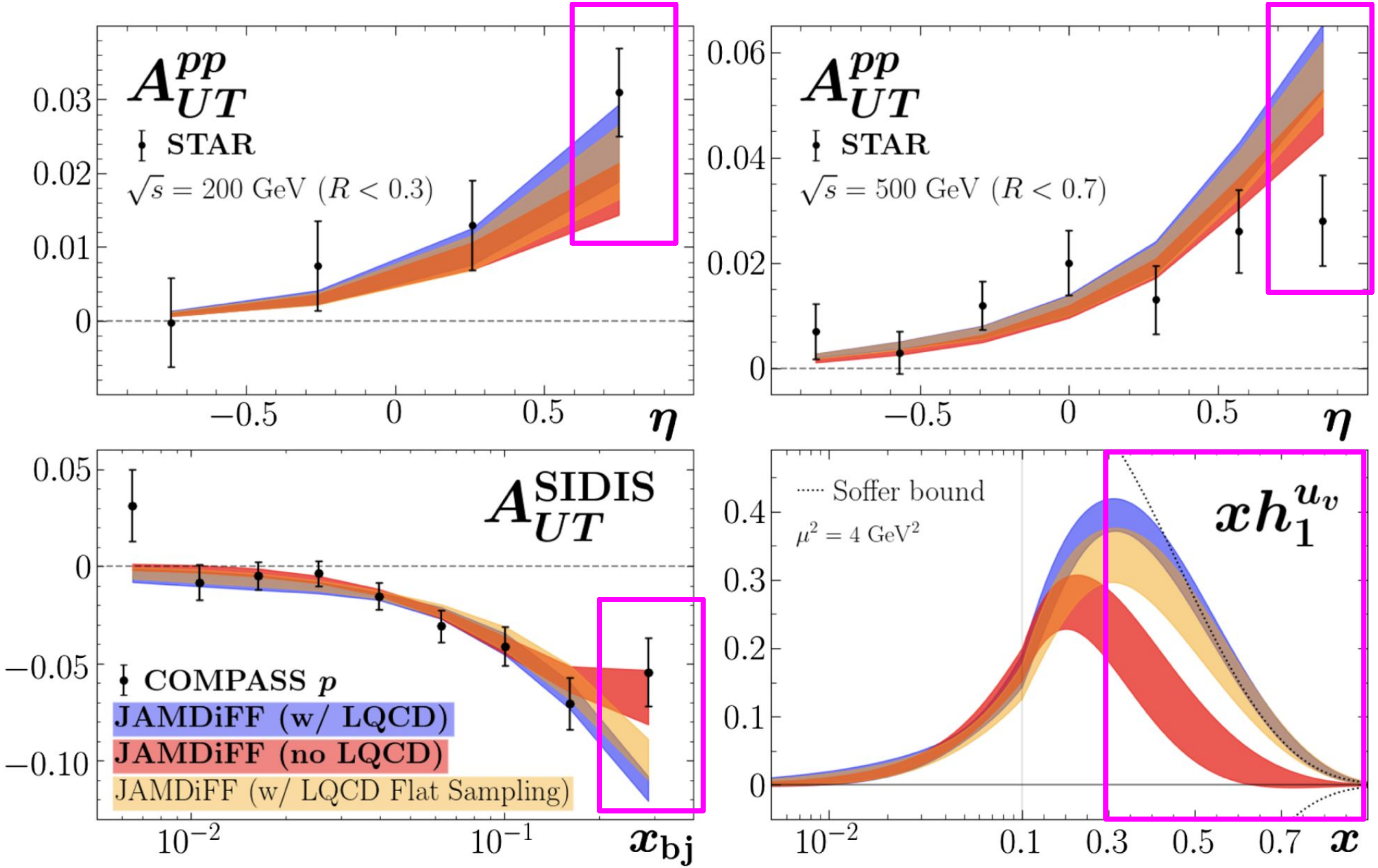

A_{UT}^{pp}
STAR
$\sqrt{s}$ = 200 GeV (R < 0.3)
η
A_{UT}^{pp}
STAR
$\sqrt{s}$ = 500 GeV (R < 0.7)
η
A_{UT}^{SIDIS}
COMPASS p
JAMDiFF (w/ LQCD)
JAMDiFF (no LQCD)
JAMDiFF (w/ LQCD Flat Sampling)
x_{bj}
Soffer bound
μ^2 = 4 GeV^2
$xh_1^{u_v}$
x

Takeaways

- At present there is no significant tension between LQCD and experimental reconstruction of nucleon tensor charges
- Different reconstructions of tensor charges are mostly driven by large x data
- More high x data is needed to reach accurate reconstruction of TPDF above x>0.3
- Inclusion of LQCD calculations as priors are very informative/useful in QCD phenomenology
- The JAMDiFF results and JAM3D* results are very similar and one can perform a combined analysis (TMD+CT3 & DiFF) **->** indicates possible **universal nature of all SSAs and nucleon tensor charges**

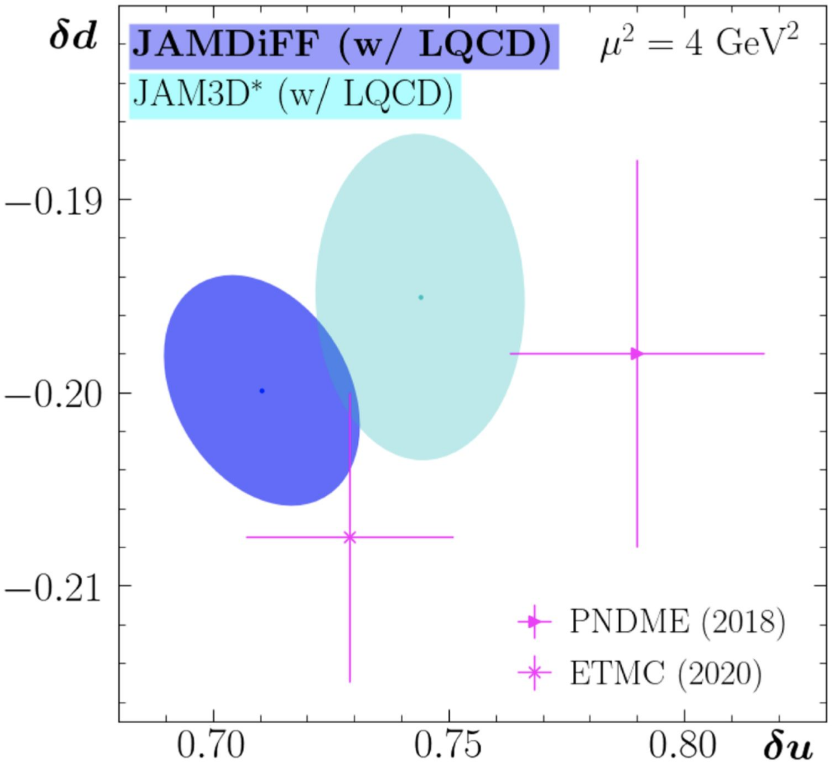

Outline

1. Gluon helicity PDF
2. Nucleon transversity/tensorcharge
3. **Pion PDF**

Cocuzza, Melnitchouk, Metz, NS '21

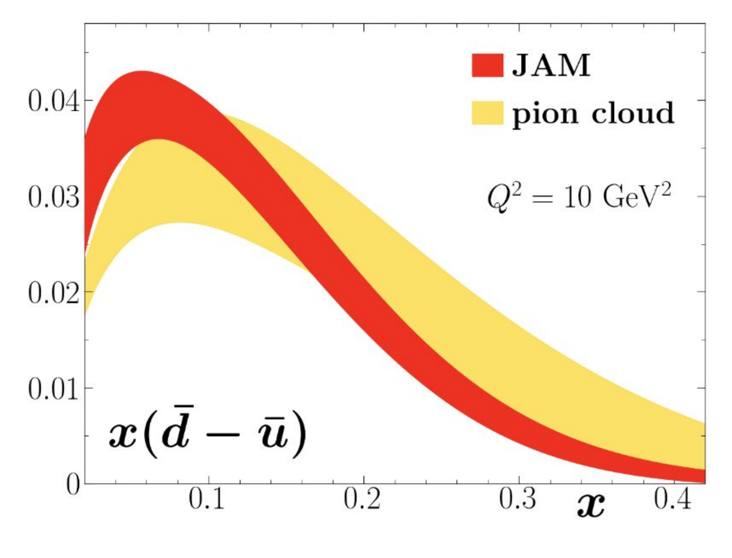

$$(\bar{d} - \bar{u})(x) = \left[\left(f_{n\pi^+} + f_{\Delta^0\pi^+} - f_{\Delta^{++}\pi^-}\right) \otimes \bar{q}_v^{\pi}\right](x),$$

Large x valence pion PDFs

Barry, Ji, Melnitchouk, NS ‘21

Aicher, Schafer, Vogelsang ‘10

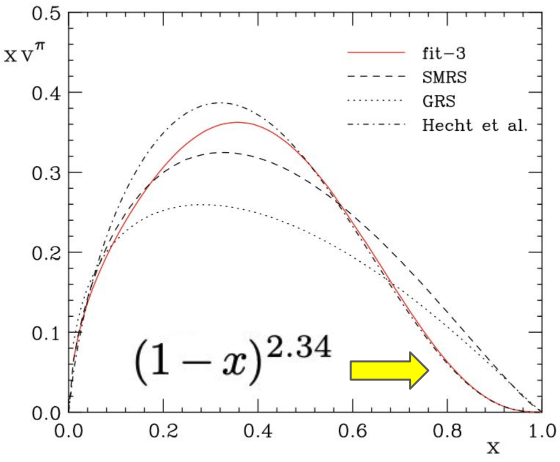

- Aicher et al, showed that large x asymptotics qV is sensitive to threshold corrections.
- Their analysis found similar asymptotic behavior as in DSE expectations.

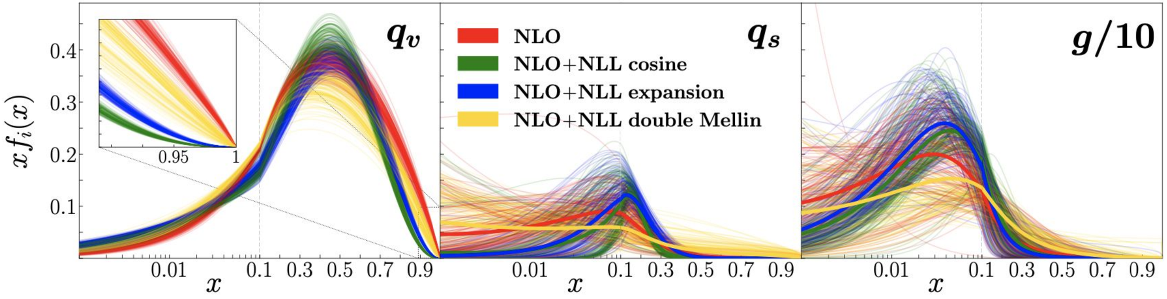

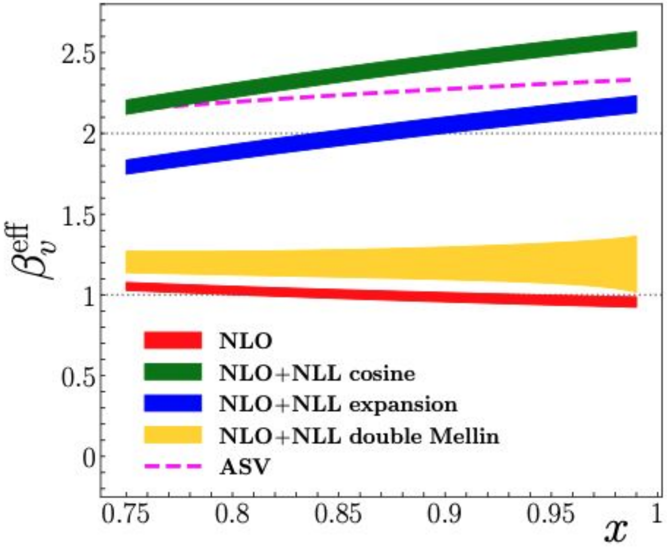

$$\beta_v^{\mathrm{eff}}(x,\mu) = \frac{\partial \log |q_v(x,\mu)|}{\partial \log(1-x)}.$$

- Improved resummation setup showed consistency of fixed order NLO results.
- DSE vs pQCD back to a disagreement

Inclusion of LQCD **JAM+HadStruc**

Barry et al. '22

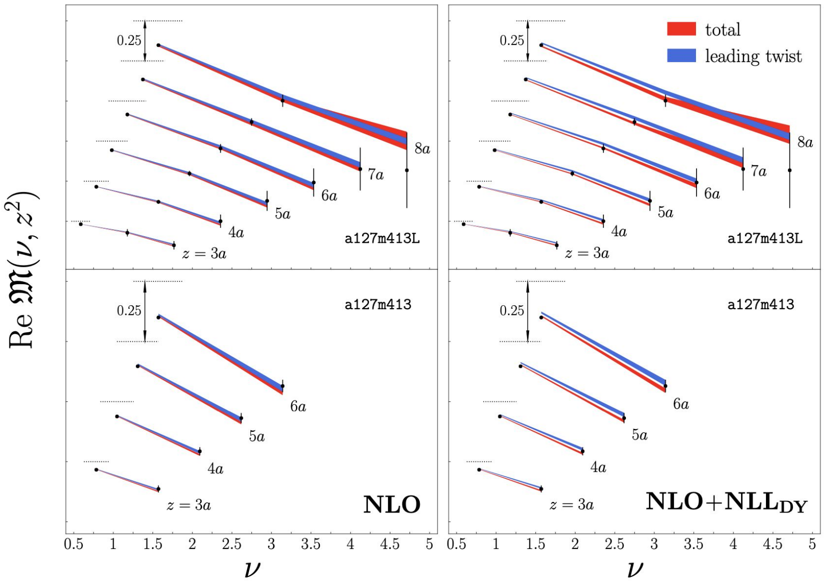

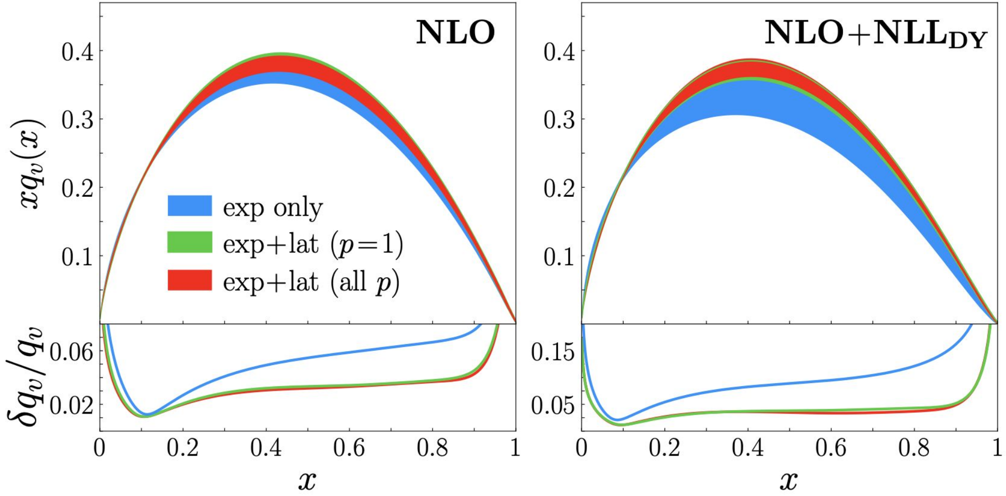

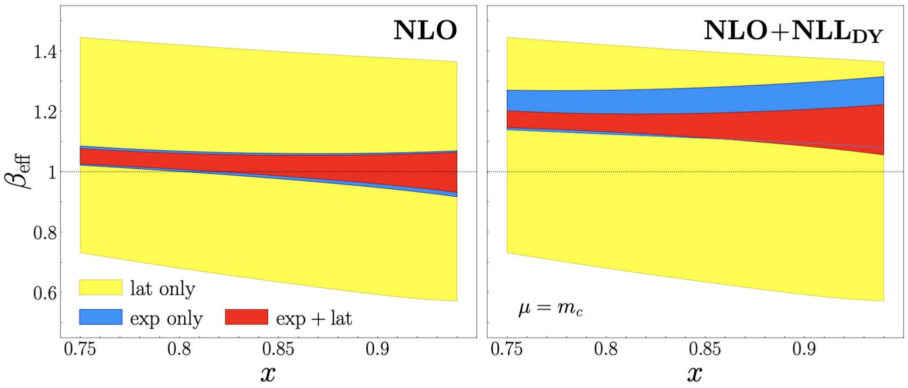

$$\mathrm{Re}\ \mathfrak{M}(\nu, z^2) = \int_0^1 \mathrm{d}x\ q_v(x, \mu_{\rm lat})\, \mathcal{C}^{\rm Rp\text{-}ITD}\left(x\nu, z^2, \mu_{\rm lat}\right) + z^2 B_1(\nu) + \frac{a}{|z|} P_1(\nu) + e^{-m_\pi(L-z)} F_1(\nu)\ .$$

An analysis of parton distributions in a pion with Bézier parametrizations

Lucas Kotz,[1] Aurore Courtoy,[2,*] Pavel Nadolsky,[1,†] Fredrick Olness,[1] and Maximiliano Ponce-Chavez[2]
[1]*Department of Physics, Southern Methodist University, Dallas, TX 75275-0175, USA*
[2]*Instituto de Física, Universidad Nacional Autónoma de México, Apartado Postal 20-364, 01000 Ciudad de México, Mexico*
(Dated: April 17, 2024)

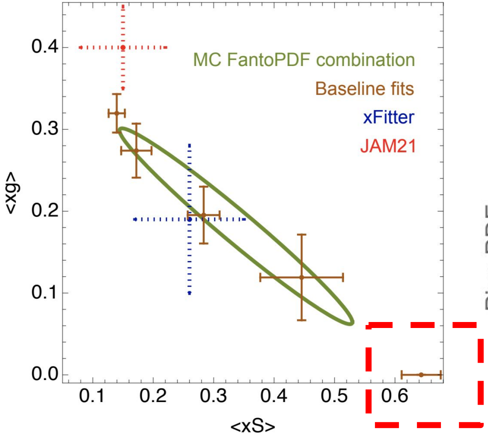

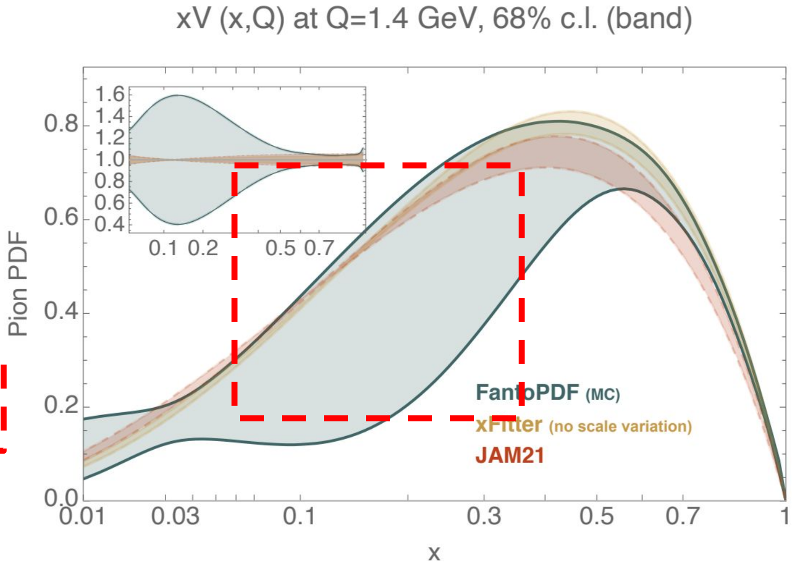

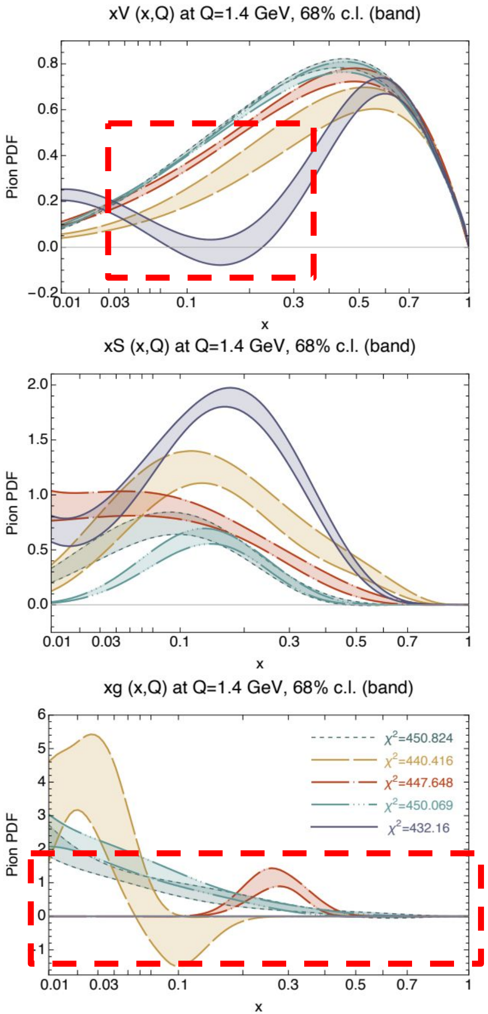

- No gluons inside pion gives best chi2
- Sea quark pdf larger than valence quark x~0.1

Toward the First Gluon Parton Distribution from the LaMET

William Good (Michigan State U. and Michigan State U., East Lansing (main)), Kinza Hasan (Michigan State U.), Huey-Wen Lin (Michigan State U.)

Sep 4, 2024

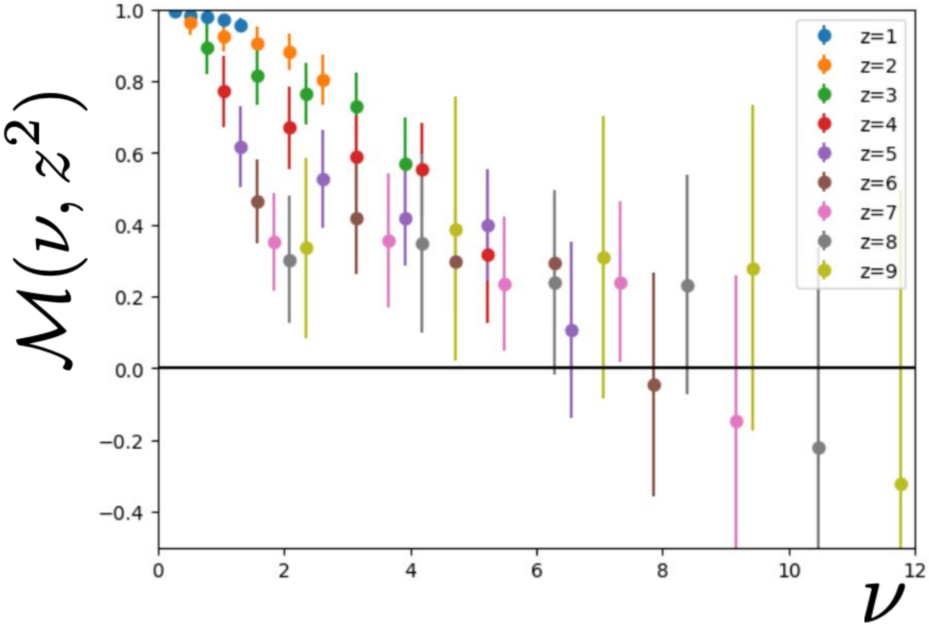

ensemble	a12m310 (310 MeV)
a (fm)	0.1207(11)
$L^3 \times T$	$24^3 \times 64$
M_π^{val} (MeV)	309.0(11)
P_z (GeV)	[0, 1.71]
N_{cfg}	1013
N_{meas}	~1.2 M
t_{sep}	[5, 9]

Reduced pseudo-Ioffe Time Distribution from one ensemble

$$\mathscr{M}(\nu, z^2) = \frac{\mathcal{M}(zP_z, z^2)/\mathcal{M}(0\cdot P_z, 0)}{\mathcal{M}(z\cdot 0, z^2)/\mathcal{M}(0\cdot 0, 0)}$$

Lattice + JAM

In collab with
Huey-Wen & Wally

Preliminary Results

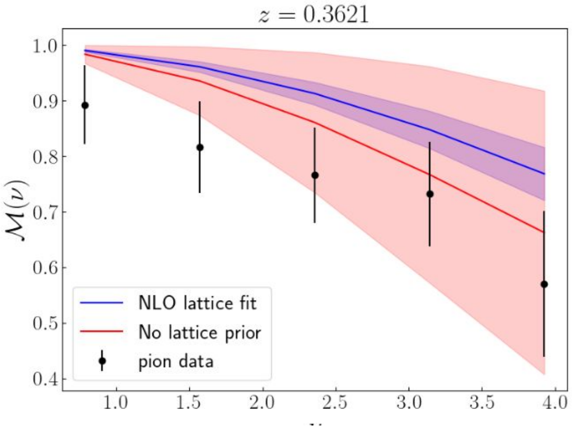

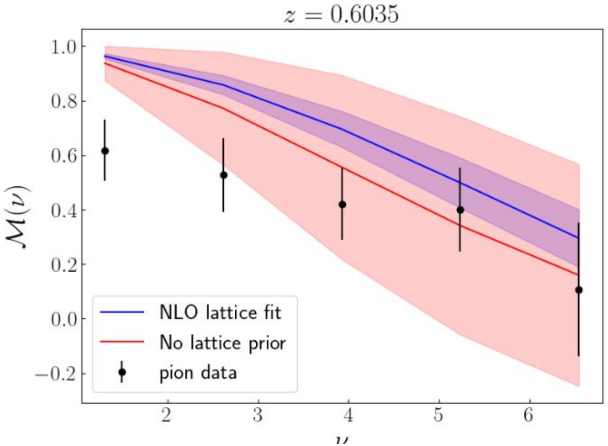

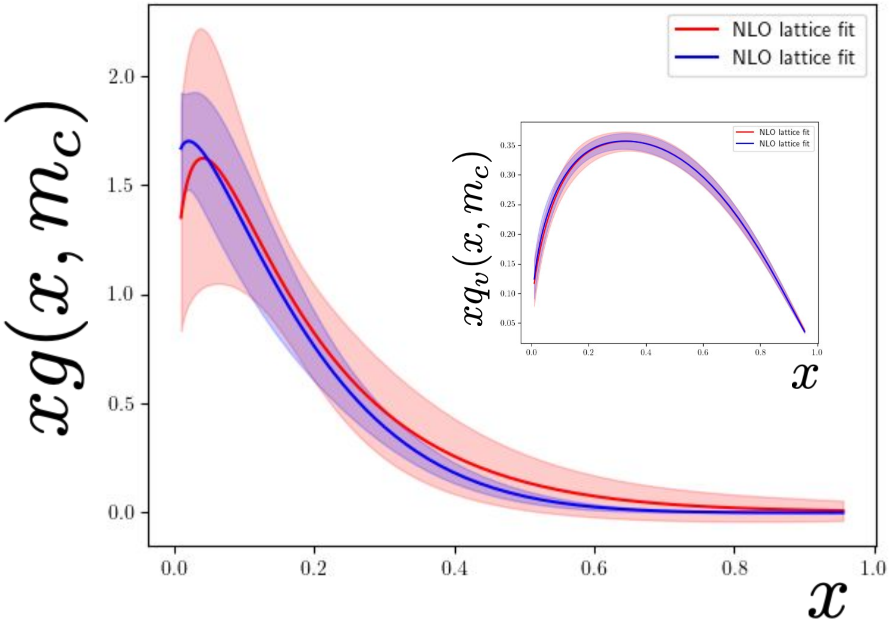

chi^2/N_pts	Before Lattice	After Lattice
Expt	0.88(5)	0.84(4)
Theory	4.3(85)	1.86(7)

- No gluons are disfavored by LQCD
- LQCD data has a strong impact relative to exp. observables

Holistic approach to QCD global analysis